

I. PHYSICAL ELECTRONICS

Prof. W. B. Nottingham
Dr. S. H. Autler
Dr. A. L. McWhorter

E. Ahilea
S. Aisenberg
D. H. Dickey
W. J. Lange

R. D. Larrabee
H. Shelton
L. E. Sprague

RESEARCH OBJECTIVES

The study of those properties of electrons that are not specifically associated with individual atoms forms the basis of the science of physical electronics. Examples of investigations carried out under this program include:

1. thermionic emission from pure materials – tungsten and complex composite surfaces, for example – including, specifically, the oxide cathode;
2. photoelectric emission from insulators and semiconductors and from pure surfaces;
3. strong field emission from single crystals and a detailed analysis of the field emission dependence on crystallographic direction and temperature;
4. properties of low-pressure gaseous discharges.

Other subjects suitable for investigation include surface properties of semiconductors, photoconductive and photovoltaic effects, and secondary electron emission from all kinds of solids, including conductors, semiconductors, and insulators.

In attempting to understand the phenomenon of thermionic emission from single crystals we decided that an investigation of the absorption process would yield certain necessary information. Two experiments were undertaken: one involves the delivery of electrons of known and very well-defined energy to a tantalum single crystal; the other involves the collimation of an electron stream by a magnetic field, and permits the investigation of both emission and absorption properties of tantalum single crystals for electrons. These experiments, that differ radically in method, are expected to yield closely related information and to establish significant new facts.

The oxide-coated cathode is economically the most important thermionic emitter at the present time. The availability of new experimental data acquired both in this and other research laboratories has made it possible to formulate a unified theory to explain the conductivity and the emission properties of these cathodes. This theory will serve as a guide to further experimental researches that are planned as an important part of our future program.

W. B. Nottingham

A. ELECTRON EMISSION PROBLEMS

1. New Method for Emission Evaluation Applicable to Oxide Cathodes

In nearly all vacuum tubes that use oxide cathodes for their source of electrons, the emission is space-charge-limited, and the desired electronic operation depends upon the modulation of the space-charge minimum by externally applied fields to obtain a controlled variation of the electron current conducted through the device. Analysis shows that little or no difference in the effective operation occurs for different cathodes if the operation does not reduce the potential difference between the space-charge minimum and the potential in the space just outside of the emitter to less than the value computed by the following equation:

$$V_s' \geq \frac{k}{q} T = \frac{T}{11600} \quad (1)$$

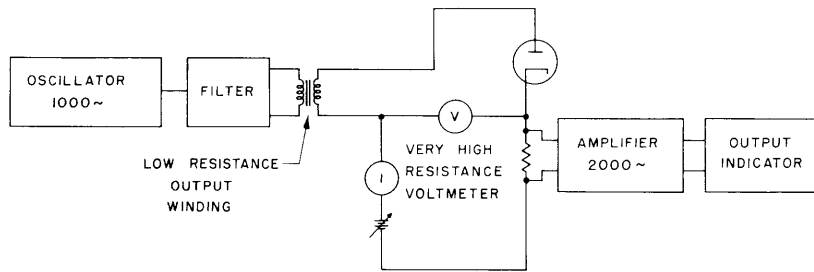


Fig. I-1. Block diagram of circuit for second-harmonic measurement.

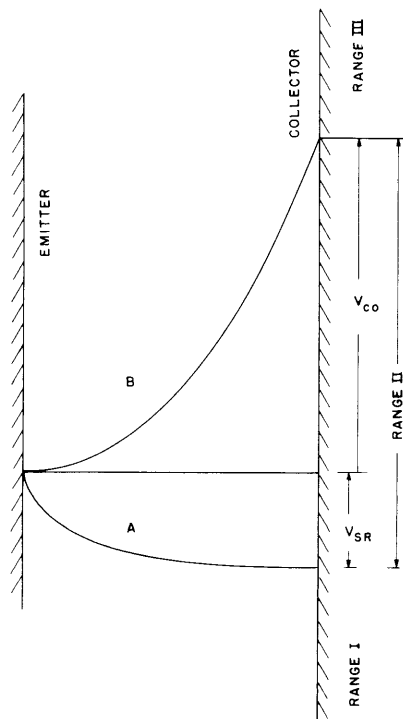


Fig. I-2. Potential distribution for two critical conditions: A is zero field at collector; B is zero field at emitter. Current is limited by space charge in range II.

(I. PHYSICAL ELECTRONICS)

The temperature of the emitter is T ; k is Boltzmann's constant, and q is the electron charge. It is a basic requirement, therefore, that any method that is truly applicable to the evaluation of emitter properties must depend upon emission current measurements with the potential minimum less than that given by V'_S of Eq. 1, preferably with the condition that the potential minimum just vanishes. This statement is equivalent to requiring that the emission capability be evaluated with zero field at the surface of the emitter.

The new method, which has been applied to the identification of this zero field condition, depends upon the measurement of the second-harmonic content of the current flowing through the device when a very small amplitude of pure sinusoidal voltage is added to the dc voltage applied to the tube. This method was described briefly in the Quarterly Progress Report of October 15, 1955. A block diagram of the circuit used is shown in Fig. I-1.

In the ideal operation of a diode there are three ranges in applied potential over which the current voltage relation follows three different laws. These ranges are best illustrated by Fig. I-2, in which two potential distributions are illustrated by lines designated A and B. Line A applies to the critical condition associated with zero field at the collector and a current being delivered to the collector of I_R . The potential difference between a point just outside the collector and a point just outside the emitter is shown as V_{SR} . There will be a certain applied potential not exactly equal to V_{SR} because of a difference in emitter and collector true work-functions that will result in this potential distribution. It is our purpose to show an easy means of determining this critical condition. As the applied potential is made more positive than this critical one, a space-charge minimum develops between the emitter and the collector; the current increases, and finally the potential distribution illustrated by curve B occurs when the field at the surface of the emitter is exactly zero and the difference in potential between points just outside of the emitter and just outside the collector is V_{CO} . The change in potential which is directly observable is the sum of these two voltages.

In experimental procedure a voltage is applied across the diode to establish a difference in potential in the negative direction which is greater than the critical value V_{SR} . This range is identified as range I, and the current across the diode will rise exponentially with the voltage. Over range I, the second-harmonic output also increases exponentially with the voltage. At the critical current I_R the law that governs the flow of electrons changes from the Boltzmann law to the space-charge law, and the second-harmonic output decreases rapidly. This very sharp maximum in the second-harmonic output establishes, without the necessity of a detailed analysis of the current-voltage curve, the applied voltage that gives the potential distribution A of Fig. I-2 and the critical current value I_R . Further increases in applied voltage result in a gradual decrease in second-harmonic output over range II. As the critical condition represented

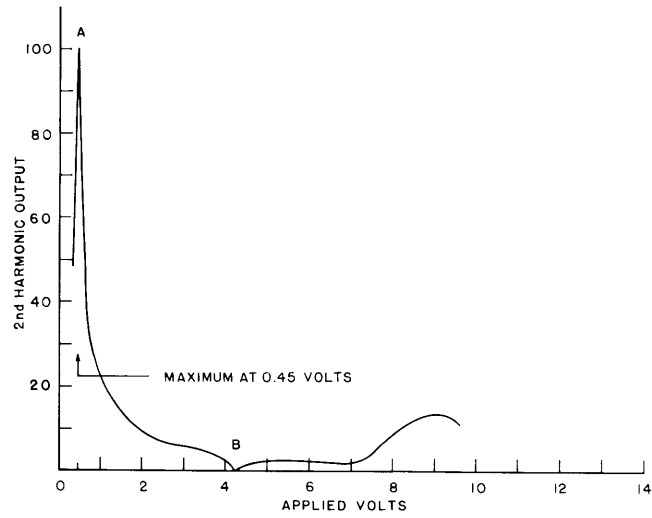


Fig. I-3. Harmonic output normalized to 100 at peak. Oxide cathode at 837°K with 3.0 volts on heater.

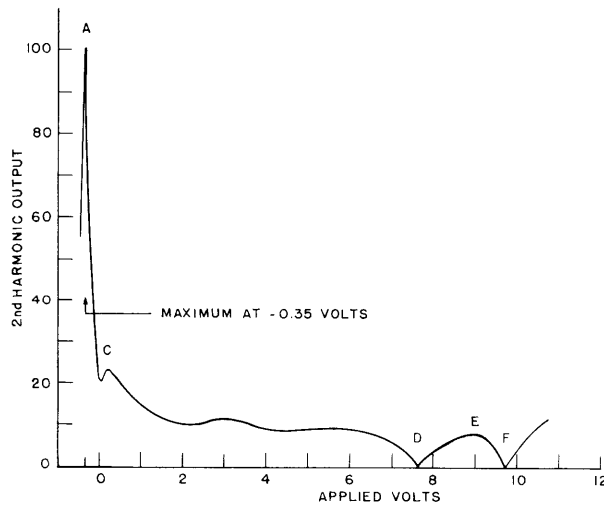


Fig. I-4. Harmonic output normalized to 100 at peak. Oxide cathode at 1160°K with 6.3 volts on heater. Space charge at A; saturated emission from uncoated parts of emitter at C; high-speed 10-volt effect at D, E, and F.

(I. PHYSICAL ELECTRONICS)

by curve B is approached, the second-harmonic output falls sharply to zero. This fact permits the quick identification of the current flowing and the applied voltage that is required at the "inflection" point of the current-voltage characteristic. This current, identified as I_0 , is an excellent measure of the useful emission capability of the cathode. This sequence of events is best illustrated by Fig. I-3, in which the corresponding critical conditions are identified by the maximum at A and the minimum at B.

Although this method of analysis can be used very simply for emitters having good uniformity and diode structures that are either the equivalent of parallel planes or concentric cylinders, complications illustrated by Fig. I-4 are likely to develop as the temperature is increased. In this figure, the onset of space-charge limitation may be clearly identified at A. There is a small minimum followed closely by a maximum at C and additional structure at D, E, and F. The diode for these measurements had a cylindrical emitter coated with barium-strontium oxide over the central part of the cathode. The total uncoated area was somewhat greater than the coated area. The purpose of this construction was to derive the electrons from the region most uniform in temperature. With the cathode at the high temperature used for Fig. I-4, the emission current measured under condition A came from the entire cathode and not just from the coated area. As the applied voltage was increased, the space-charge minimum developed, and the current demand from the uncoated area was so great that the space-charge minimum moved across the tube and created the potential distribution of curve B, Fig. I-2, in the regions outside the coated area. This transition was responsible for the structure at C.

Matheson and Nergaard (1) have described the "high-speed ten-volt effect" which results from the emission of secondary electrons from the collector in sufficient number to contribute measurably to the space-charge in its immediate neighborhood. The presence of these electrons shows up as a sharp decrease in the second-harmonic output at D. A maximum occurs between D and F as the number of electrons in this space-charge cloud increases, but at F the rate of increase falls and a second minimum occurs beyond which the second-harmonic output does not change sharply.

These studies were made with a General Radio wave analyzer for the separation and measurement of the second-harmonic output. An analyzer that not only permits the measurement of the amplitude but also the phase of the output would make the analysis of the more complex characteristics more satisfactory. Measurements made and properly interpreted for a range in emitter temperature will give data by which an excellent evaluation of the emitter properties can be obtained.

W. B. Nottingham

References

1. R. M. Matheson and L. S. Nergaard, RCA Rev. 12, 258 (1951).

(I. PHYSICAL ELECTRONICS)

2. Reflection of Slow Electrons at a Metal Surface

Some interesting data were obtained on the reflection of slow electrons at a metal surface. To date, experiments have been done by retarding potential methods. The source of nearly monoenergetic electrons is a magnetic velocity analyzer. Using it to measure e/m , the operation of the analyzer was checked by observing the applied potential required to bring the maximum current around the analyzer, as a function of magnetic field. By extrapolation, this experiment yielded 0.1 volt as the value of the applied potential between the tungsten filament and the tantalum analyzer for zero magnetic field. Since the tungsten filament is a single crystal oriented with the 116 direction facing the analyzer, its work-function can be used as a reference point for finding other work-functions. Hutson's data (1) give $4.25 + 3 \times 10^{-5}T$ for this surface. The distribution of electrons leaving the filament was determined experimentally. This showed that the electron energy at maximum emission was about 0.25 ev. From these facts the work-function of the analyzer could be fixed at 4.65 ev.

When the electron beam leaves the analyzer it can be either accelerated or decelerated between the exit slit and the metal surface to be studied. The geometry is plane parallel, so that the electron trajectories are known. The metal surface is a single crystal of tantalum with a 110 surface exposed.

Figure I-5 shows the results obtained when the energy of the electron beam at the

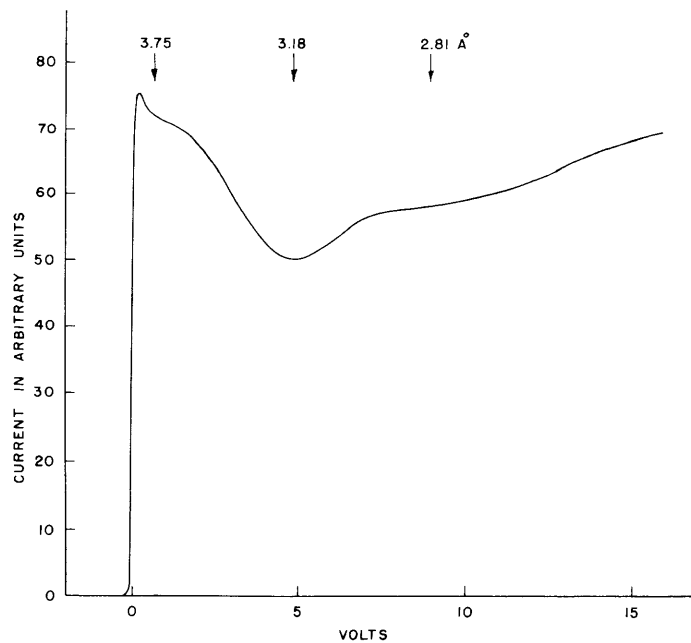


Fig. I-5. Current collected by tantalum crystal versus applied potential – filament to target.

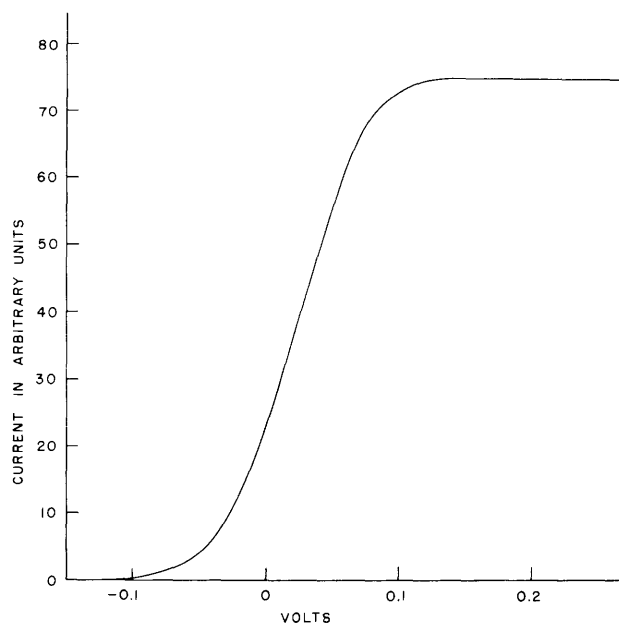


Fig. I-6. Expanded scale of Fig. I-5 near zero.

surface is varied from zero to 15 volts. The marked electron wavelengths were calculated with the use of an electron affinity W_a (work-function plus Fermi energy) equal to 10 ev. The main features of the curves are independent of whether the region between the exit slit and target is accelerating or retarding. They are also independent of whether the target has been flashed to 2100°K within 7 minutes of the voltage run or permitted to adsorb gases for months. As the target was flashed the ionization current in the gauge remained constant, indicating a vacuum of 7×10^{-9} .

The voltage region in which the electrons are retarded to the point of stopping just at the metal surface was examined more closely and is shown on an expanded voltage scale in Fig. I-6. The symmetry of the curve about its half-value point seems to indicate a nearly triangular resolution.

W. J. Lange

References

1. A. R. Hutson, Phys. Rev. 98, 889 (1955).

B. PHYSICAL ELECTRONICS IN THE SOLID STATE

1. Hall Effect in Lead-Sulfide Films

More equipment for the measurement of the Hall effect in films of lead sulfide was constructed. Copper-constant thermocouples were calibrated for temperatures over

(I. PHYSICAL ELECTRONICS)

the range of that of liquid nitrogen to +100°C and are now satisfactory for the sample temperature regulation and measurement. Heater wires were wound on the copper cylinder which surrounds the glass sample bottle. Teflon tubing was used to insulate the heater wires electrically from the copper cylinder. Teflon can withstand a temperature as great as 250°C, which is higher than that reached by the heater wires. A magnetometer designed for this work (described in Section I-D.1 of this report) was tested and proved adequate.

At the present time, preliminary work is being carried on in the design of a dc millivoltmeter capable of measuring the Hall potentials at an input impedance large compared with that of the samples, which often have a resistance exceeding 10^{12} ohms at low temperatures.

D. H. Dickey

2. Electric Properties of Ion-Bombarded Germanium Surfaces

Preliminary measurements of resistance, field effect, and photoconductivity were made on 100-oriented surfaces of near-intrinsic n-type germanium samples that were subjected to the cleaning procedure developed by the Brown University group (1). The samples were outgassed at about 600°C for about 60 hours in vacuum ($<10^{-8}$ mm) by passing current through spot-welded molybdenum contacts. Argon-ion bombardment increased the resistance more than 25 per cent and greatly reduced the field effect and photoconductivity. Upon annealing, the resistance decreased to less than its pre-bombardment value and the photoconductivity recovered substantially. The field effect increased markedly and had a flat frequency response from 10 to 1000 cps, with a sign indicating a p-type surface. Exposure of the sample to oxygen at a pressure of about 10^{-3} mm caused the resistance to increase nearly 50 per cent, while the photoconductivity decreased or remained the same, depending on the sample. The amplitude of the field effect increased by a factor of 2 or 3, with the frequency dependence and sign remaining unchanged. These changes occurred over a period of minutes when the surface was exposed to oxygen, indicating that the rate is not determined by the oxygen pressure.

The observations are consistent with previous electron diffraction (1) and surface recombination (2) studies, which may be interpreted by assuming that the bombardment leaves the surface chemically clean but physically rough, while annealing produces a clean, regular surface. More work will be done to determine the optimum conditions for bombarding and annealing, and more precise measurements will be made on various samples.

S. H. Autler, A. L. McWhorter

References

1. H. E. Farnsworth, R. E. Schlier, T. H. George, and R. M. Burger, J. Appl. Phys. 26, 252 (1955). Also Quarterly Progress Reports, Group 35, Lincoln Laboratory, M.I.T., 1955, 1956.
2. H. E. Farnsworth, private communication.

3. Surface Studies on Semiconductors

For measuring the contact potential of a small ($2.5 \text{ cm} \times 0.5 \text{ cm}$) sample of germanium, the method of retardation of an electron beam is now considered more suitable than the Kelvin method for the following reasons: (a) photoconductivity measurements can be made simultaneously with contact potential measurements which may be required by the experiment; (b) the difficulty of small size in designing apparatus for the Kelvin method is eliminated; (c) the electron-emitter surface can be kept clean by its own heat, as changes in the ambient and treatments of the germanium surface are required by the experiment. Precaution must be taken, however, to prevent the light and the electron emitter from illuminating the germanium. The design of the tube incorporates a simple electron accelerator, pointed away from the germanium, and a means of deflecting the electron beam toward the germanium (without, of course, deflecting the light coming from the emitter).

E. Ahilea

C. GASEOUS DISCHARGES

1. Ion Generation, Distribution Functions, and Probe Measurements

The theory of the harmonic analysis of current-versus-voltage characteristics of thermionic tubes, described by Prof. W. B. Nottingham in the Quarterly Progress Report of October 15, 1955, page 10, has been extended to the point where the equivalent temperature of a Boltzmann distribution can be easily obtained from an ac and a dc meter reading with the use of relatively simple equipment. This method will not only indicate the existence of a Boltzmann distribution and give the corresponding temperature but it will also permit the measurement of more general distribution functions. The plasma potential is also easily located with the same equipment.

Construction of a temperature-regulating water bath for the mercury vapor discharge tube was completed, and some of the necessary electrical measuring equipment was obtained. Construction and design of additional measuring and regulating equipment is progressing.

Special multiple probes and hollow probes are being designed for accurate measurement of ion generation in the mercury arc plasma.

S. Aisenberg

(I. PHYSICAL ELECTRONICS)

D. EXPERIMENTAL TECHNIQUES

1. Null Rotating Coil Magnetometer

In order to measure magnetic fields greater than 500 gauss, nonuniform to the extent of 2 per cent per square inch, to an accuracy of 1 per cent or better, a null rotating coil magnetometer was conceived, designed, constructed, and tested.

The basic idea is that of generating and adding two 30-cps signals, one proportional to an unknown field, and another equal in magnitude but 180° out of phase, produced by a standard solenoid. The solenoid current required to set up the "bucking" signal is a measure of the unknown field. Any small difference between the signals is detected by a 30-cps peaked amplifier and an oscilloscope. This difference is nulled by adjusting the solenoid current and the phase between the two signals (Fig. I-7). The relative phase between the signals is set to 180° by adjusting the angular position of the solenoid coils in a plane perpendicular to the drive shaft. The peaked amplifier is used to filter out the harmonics generated in a magnetic field that has nonuniformities in a plane perpendicular to the axis of rotation.

To prevent stray fields from influencing the standard field, a double Mumetal shield was placed around the standard solenoid and its associated pickup coil. Hysteresis effects cause an error of less than $1/3$ gauss upon momentarily placing the Mumetal shield in contact with a 5000-gauss magnet.

The standard field arises from a current that is accurately measured by a potentiometer. This magnetometer will be calibrated against a resonant-probe magnetometer in a uniform field.

Tests on the instrument, carried out during one month, showed an instability of less than 0.5 per cent and a short-term reproducibility of better than 0.2 per cent. Since the

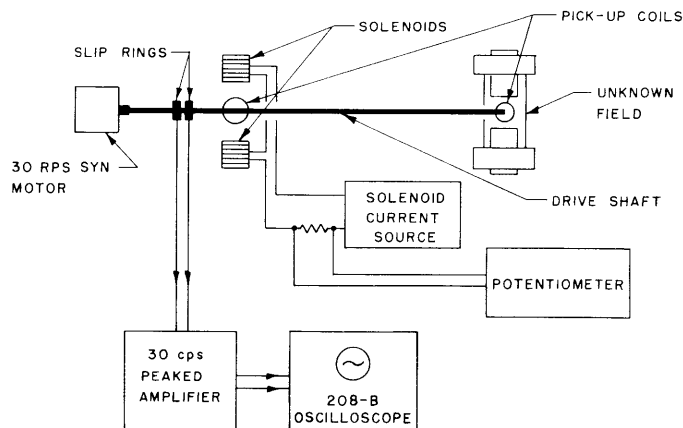


Fig. I-7. Null rotating coil magnetometer.

(I. PHYSICAL ELECTRONICS)

detection sensitivity is about 1 gauss, fields as low as 100 gauss can be measured to 1.0 per cent. The maximum allowable current through the solenoid determines the maximum field that can be measured. This current was found to be about 100 milliamperes, so that the present instrument is limited to fields of about 4000 gauss. To allow the measurement of larger fields, the unknown pickup coil may be modified.

Details of the magnetometer design are as follows. A small synchronous motor having a torque of 0.4 in-oz is used for the drive power. The drive shaft is a 1/8 inch nonmagnetic stainless steel tube held in oil-impregnated sleeve bearings mounted in a 3/8 inch nonmagnetic stainless steel tube. The "unknown" pickup coil is about 5/32 inch (diameter) \times 3/16 inch; the reference pickup coil is 3/4 inch (diameter) \times 1/8 inch; both are wound with 0.001 inch (diameter) Formex covered copper wire (No. 49 AWG). The distance between pickup coils is about 32 inches. The steel shaft is used as one lead between the pickup coils; the other lead passes down the center of the tubular shaft. Slip rings of silver and brushes of graphite are used. All materials, other than the Mumetal shields, are brass, nonmagnetic stainless steel, or some other nonmagnetic material. The synchronous motor, made of magnetic material, is mounted outside the Mumetal shield, removed by a distance of about 8 inches. Each solenoid is 3/4 inch (diameter) \times 1 1/4 inches wound with No. 26 magnet wire. All coils are wound on linen bakelite forms.

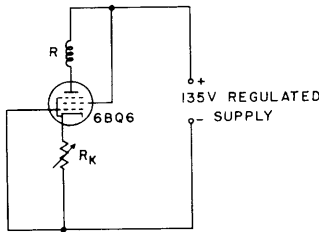


Fig. I-8. Solenoid current regulator.

To provide a more constant solenoid current as the solenoid resistance changes because of heating, the cathode follower in Fig. I-8 is used. R represents the solenoids, and R_K is a series potentiometer used to adjust the solenoid current. The drift accompanying changes in R or in the supply voltage is decreased at least by a factor of 100, the exact amount depending on the value of R_K . The smaller the current, the higher the value of R_K will be, and the greater the feedback.

D. H. Dickey

2. Ionization Gauge Control Circuit

Work was completed on the final form of a new circuit designed for use in conjunction with ionization gauges for the convenient measurement of very low pressures.

The most important feature of the circuit is a stable dc amplifier that features both positive and negative feedback. The principle of operation of the dc amplifier is

(I. PHYSICAL ELECTRONICS)

shown in Fig. I-9. It can be shown that

$$\frac{e_o}{R_{g^+} i_+} = \frac{A_1 A_2 A_3}{1 - \gamma A_1 A_2 - \beta A_1 A_2 A_3} \left[1 + \frac{1}{R_{g^+} i_+} \left(\delta_1 + \frac{\delta_2}{A_1} + \frac{\delta_3}{A_1 A_2} \{1 - \gamma A_1 A_2\} \right) \right]$$

For the usual case, where $\beta A_1 A_2 A_3 \gg 1 - \gamma A_1 A_2$, this reduces to

$$\frac{e_o}{R_{g^+} i_+} \cong -\frac{1}{\beta} \left[1 + \frac{1}{R_{g^+} i_+} \left(\delta_1 + \frac{\delta_2}{A_1} + \frac{\delta_3}{A_1 A_2} \{1 - \gamma A_1 A_2\} \right) \right]$$

which demonstrates that the negative feedback results in a relation between the output voltage e_o and the unknown ion i_+ current, which is very independent of the amplifier gain.

The quantities $\delta_1, \delta_2, \delta_3$ correspond to the various causes of zero drift. Variations of the voltage-regulator tube which supplies the filament current for the electrometer pentode are the major cause of δ_1 , which is less than approximately 10 mv. This corresponds to a zero shift of about 1 per cent of full scale but usually occurs only when a spark coil or rf induction heater is operated nearby. In the absence of gross disturbances of the voltage-regulator tube, this cause of drift is usually less than 0.3 per cent, once the various tubes are aged. Use of a USN OA2 WA tube in place of the standard OA2 voltage-regulator tube results in an even more stable zero. The quantities δ_2 and δ_3 are predominantly caused by changes of filament voltage in the cathode-follower tubes. A change of line voltage of ± 10 per cent results in an equivalent signal at the grid of about 200 mv with a 12AT7 tube, corresponding to a zero drift of about 0.3 per cent. Note that the positive feedback reduces somewhat the zero drift of the circuit.

The time constant of the circuit is also reduced by the feedback, since the ratio of

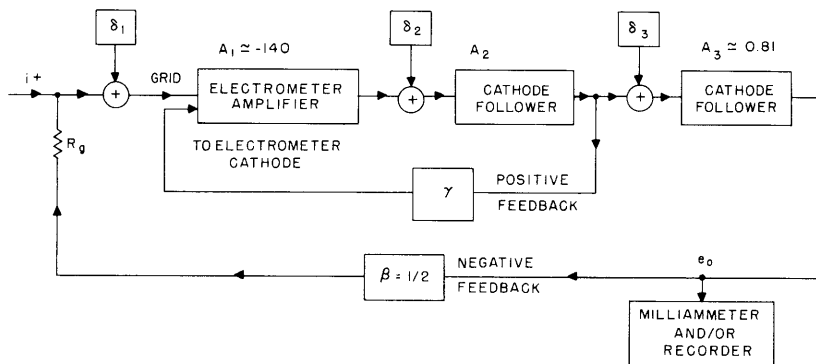


Fig. I-9. Block diagram of dc electrometer amplifier.

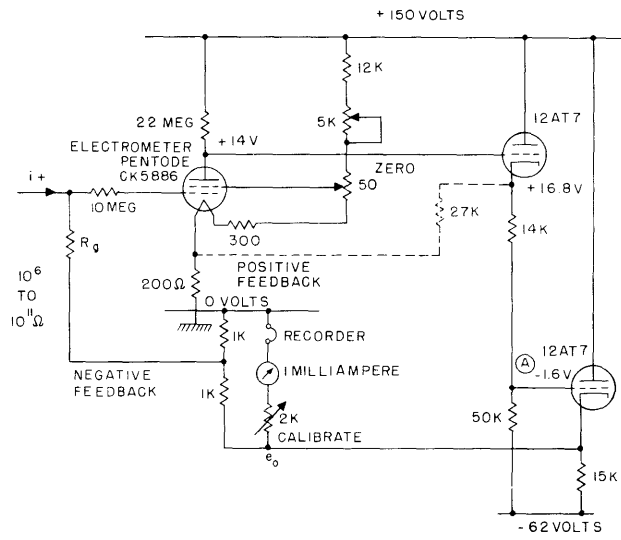


Fig. I-10. Circuit diagram of dc electrometer amplifier.

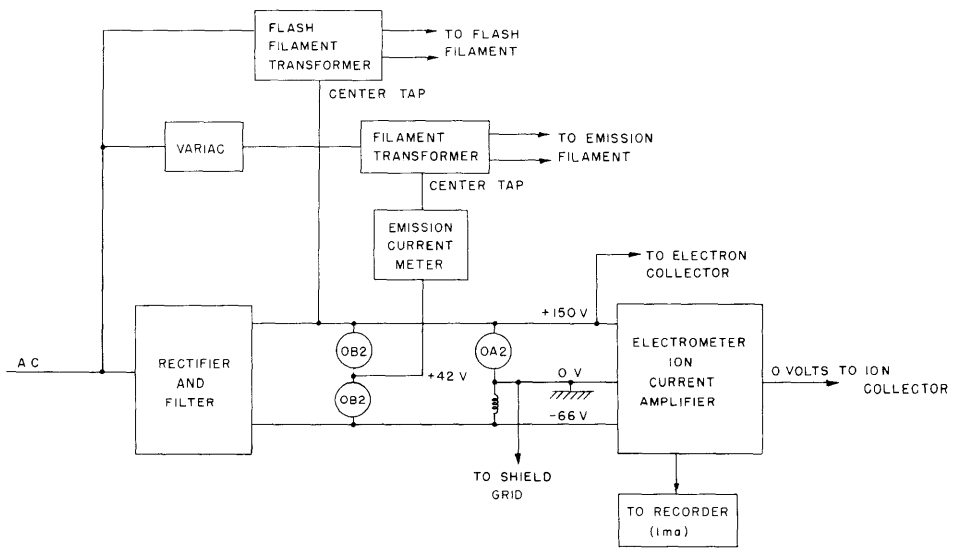


Fig. I-11. Ionization gauge control circuit.

(I. PHYSICAL ELECTRONICS)

the time constant with feedback τ' to the time constant without feedback τ is approximately given by

$$\frac{\tau'}{\tau} = \frac{1 - \gamma A_1 A_2}{1 - \gamma A_1 A_2 - \beta A_1 A_2 A_3} \approx \frac{1}{160}$$

Without positive feedback ($\gamma=0$), the time constant is reduced by a factor of about 40, but with some positive feedback ($1 - \gamma A_1 A_2) \approx 1/4$, an additional improvement of a factor of about 4 is obtained. In addition, the improved feedback yields a voltage sensitivity of about 6 mv full scale. Since the positive feedback is achieved by the use of only one additional resistor, the improvement is well worth the effort. Both the positive and negative feedbacks are obtained without using batteries.

A more detailed circuit diagram is given in Fig. I-10. The use of the second cathode follower permits the operation of a milliammeter or recorder with overload protection without losing more than a factor of 4 in the negative feedback loop that would occur if the output and feedback voltages were obtained from point A (as was done in a previous circuit of mine). The principle of operation of the complete ionization gauge control circuit is illustrated in Fig. I-11.

Other features and advantages of this ionization gauge control circuit will be described later.

S. Aisenberg

3. Spectral Emissivity of the Refractory Metals

An experiment designed to measure the spectral (optical) emissivity of the refractory metals as a function of wavelength and temperature is in progress. The basic vacuum tube (see the Quarterly Progress Report of January 15, 1955, pp. 3-4) designed for studying the evaporation rate of tungsten and any impurities at high temperatures and for measuring subsequently the spectral emissivity is nearing completion.

R. D. Larrabee